



Synthesized Schiff bases from linoleic and benheric acids as inhibitor of mild steel corrosion in HCl medium

Ekuma F.K. *, Odoemelam S.A., Ekanem U.I. and Okoyeagu A.

Department of Chemistry, Michael Okpara University of Agriculture, Umudike, Abia State, Nigeria
popefrank2013@yahoo.com

Available online at: www.isca.in, www.isca.me

Received 30th June 2018, revised 18th August 2018, accepted 19th September 2018

Abstract

Inhibitory performances of Schiff bases, 2[2-diethylamino) ethyl methyl amino)-4-methyl-5-3 (3-methyl sulfanyl propyl amino) methylidene cyclohexdien-1-one (DEMS) and [1-(azepan-1-yl)-2-2-[4-(2-tert-butyl sulfanylethyl piperazin-1-yl)] ethanone (ATSP) synthesized from linoleic and benheric acids on mild steel corrosion in HCl medium were assessed. Inhibition performances of the Schiff bases under study were assessed by gravimetric and potentiodynamic polarization methods. The inhibitors were characterized by Infrared (IR) spectrophotometry. Results obtained showed pronounced enhancements in efficiencies of the inhibitors as their concentrations gradually increased while a corresponding decline in efficiencies was observed with a rise in temperature of the medium. The measured corrosion data were best described by Langmuir isotherm with R^2 values of 0.99. Thermodynamic studies on the inhibition process showed that the mode of adsorption of the Schiff bases followed physisorption. The negative entropy values obtained revealed increased disorderliness at the mild steel-inhibitor interface as concentrations of the Schiff bases gradually build up. Potentiodynamic polarisation results revealed that the inhibitors exhibited a mixed inhibition control.

Keywords: Adsorption isotherms, corrosion inhibitors, inhibition efficiencies, Schiff bases, weight loss.

Introduction

Metals are common substances that are utilized both at home and in the industries. Their usages range from extraction industries, manufacturing industries and production industries and are also used in the production of machines used in various forms of industrial purposes. Despite their extensive applications in these industries, their liability to degradation in atmospheric air containing water vapour and their fast deterioration rate in acidic or alkaline medium are the major demerits in their applications on larger scale. Steel, an alloy made from a mixture of two or more metallic elements and/or non-metallic elements, despite its economic and industrial importance has problems associated with corrosion and this continues to constitute an issue of immense concern as corrosion tends to reduce the life span of this metal if not properly protected. Over the years, corrosion of metals has led to huge losses of artificial and natural resources annually. In the oil and gas industries, more than half of the reported cases of pipelines failures are attributed to corrosion.

Due to the problems associated with corrosion with respect to metals, the qualities of metals can be improved by employing strategies which could retard or greatly inhibit reactions at the anodic and/or cathodic regions of metallic surfaces thereby minimizing corrosion. The various methods used in minimizing corrosion in metals include: cathodic protection¹, anodic protection², coating³, alloying, plating, use of chemical inhibitors⁴⁻⁶ etc. According to Hosseini *et al.*⁷, corrosion can best be controlled by the inclusion of small amounts of inhibitor

compounds into the corrodents, and such compounds have been found to alter both cathodic and or anodic reaction and will consequently retard corrosion rate. The application of inhibitors to corroding medium has shown to be an effective way of protecting metals against corrosion⁸. In the search for various ways of checkmating the problem of corrosion in our environment, consideration is not only limited to the type of inhibitor used, but also on the effects of such inhibitors on the environment. Schiff bases, which are environmentally friendly organic inhibitors double up as mixed- type inhibitors and this attribute makes them more preferable to inorganic inhibitors. These unique attributes of Schiff bases form the basis of the present research work, which centre on the assessment of the inhibitory performances of Schiff bases synthesized from linoleic acid and benheric acid on mild steel corrosion in aqueous HCl.

Materials and methods

Mild steel used in the present investigation was pressed-cut into 3 cm by 3cm dimension. Each coupon was sand-papered using different grades of sand papers (rough and then smooth) until a mirror polished surfaces were obtained. The surfaces of the coupons were washed with ethanol to remove any stains or grease, later washed with de-ionised water and then cleaned with acetone. They were finally air-dried for some hours before been kept in a desiccator. Varying concentrations of the Schiff bases (0.2g/l, 0.4g/l, 0.6g/l, 1.0g/l and 2.0g/l) employed in the study were prepared in 1 M concentration of HCl.

Synthesis of the Schiff bases: Preparation of methyl esters from oils: Methyl esters were prepared from the linoleic and benheric oils by acid catalyzed esterification method according to Toliwal *et al.*⁹. Exactly 100g of the oil was weighed into a 500 ml round bottomed flask then followed by the addition of 300 ml of methanol and 1ml of concentrated tetraoxosulphate (VI) acid into the flask. The content was refluxed for 4h in a thermostated water bath, thereafter the unreacted methanol distilled over followed by the addition of 50ml of distilled water. A separating funnel was used to separate the contents of the flask into a lower aqueous layer and an upper organic layer. The organic layer of the immisible mixture was extracted and washed three times with 1% solution of Na₂CO₃ to remove un-esterified fatty acids and the esters were finally purified by distillation.

Preparation of fatty acid Hydrazide: Fatty acid hydrazide was prepared by measuring 0.1M fatty acid ester into 150ml ethanol in a refluxing flask, followed by addition of 0.2M hydrazine hydrate (95%) into the mixture. The contents were refluxed for 4h and cooled. The residue was washed and then separated from ethanol by recrystallization. Further, a solution of 0.02M fatty acid hydrazide in 50ml methanol was prepared using the method stated in Toliwal *et al.*⁹. A solution of 0.03M potassium thiocyanate and 3ml of concentrated HCl were added with constant stirring into the round bottom flask. The mixture was evaporated to dryness immediately on a steam bath and then heated for an additional one hour with 150ml ethanol. The resulting solid was mixed with 10ml of distilled water and 20ml ethanol and then separated from ethanol by recrystallization.

Schiff base preparation: The Schiff bases under investigation were prepared by adding to a solution of 0.02M acetaldehyde in absolute alcohol a 0.02M thiosemicarbazide according to Yaseen *et al.*¹⁰ and the mixture refluxed for 7h on a water bath. The contents were cooled and filtered and then separated from ethanol by recrystallization. The Schiff bases were characterized using FTIR spectrophotometer.

Corrosion studies: Weight loss technique: The pre-weighed coupons were suspended vertically in a 100ml of 1.0M HCl in which the Schiff bases under study had been introduced for a period of 3h. At the end of every 3h, the coupons were withdrawn with the aid of a fishing line hung through the holes bored at their upper edge and then transferred into the washing solution to quench the corrosion process. The metal coupons were scrubbed and washed thoroughly with a distilled water. The coupons were dried and re-weighed to determine the difference in weight in grams. The inhibition performances of the Schiff bases were also investigated as a function Temperature (303K to 343K) and results obtained from the mean weight loss were used to calculate corrosion rate using the relation expressed in equation-1.

$$\text{Corrosion rate} = \frac{\Delta W}{At} \quad (1)$$

Where: ΔW is weight difference in grams, A is surface area of the metal coupon in cm² and t is the immersion time in hour.

The surface coverage and the percentage inhibition were calculated by the relations given in equations (2) and (3).

$$\theta = \left(\frac{CR_0 - CR_1}{CR_0} \right) \quad (2)$$

$$(I\%) = \left(\frac{CR_0 - CR_1}{CR_0} \right) \times 100 \quad (3)$$

Where: CR_1 and CR_0 are the corrosion reaction rates with and without the Schiff base inhibitor molecules respectively.

Electrochemical polarization measurement: Electrochemical polarization measurement was done in a conventional three electrode cell consisting of the corroding specimen (mild steel) as the Working Electrode (WE), a platinum Counter Electrode (CE) and a Saturated Calomel Electrode (SCE) as the reference electrode.

The metal coupons were subjected to varying concentrations of the inhibitors in 250ml of the 1.0M HCl at 303K. The corrosion current densities were estimated from the extrapolated Tafel polarization plots using the relation given in equation-4.

$$I\% = \frac{(i_{corr} - i_{corr(inh)})}{i_{corr}} \times 100\% \quad (4)$$

Where: i_{corr} and $i_{corr(inh)}$ represent corrosion current densities in the blank and in different concentrations of the Schiff base inhibitors, respectively.

Results and discussion

Fourier transform infrared spectroscopy: The Schiff base (inhibitor) molecules were characterized using infrared (IR) spectrophotometer. The IR spectra of the Schiff bases were measured using a Perkin-elmer-1600 FT-IR spectrophotometer with resolving power of 4cm⁻¹.

The common features of the FTIR spectra of the studied compounds (Schiff bases) show bands at the range of 1760 to 1735cm⁻¹ indicating the presence of C-C and C=O stretching, bands of esters and the carboxylic groups having the wave number ranges 3300-2500cm⁻¹. The absorption bands in the range of 2260cm⁻¹ to 2220cm⁻¹ show presence of Nitrile (C≡N). Strong bands around the wave number range 1650-1560cm⁻¹ show the presence of NH₂ (amide) stretching vibration. The strong absorption broad sharp bands around 3600-3200cm⁻¹ could be attributed to the presence of -OH (alcohol/phenol) stretching vibration. The wave number ranges, 2950-2850cm⁻¹ are associated with the stretching of alkyl -CH- vibration. The wave number stretch with the range 1740-1690cm⁻¹ is associated with aldehyde (-CO) stretch. The bands, 3500-3300cm⁻¹ show primary and secondary amides. Of special interest in the study is

the strong absorption bands at $1550\text{--}1460\text{cm}^{-1}$ and $1300\text{--}1100\text{cm}^{-1}$ which are associated with secondary amide and primary amide (NH_2) with wave number ranges $1200\text{--}1050\text{cm}^{-1}$, and the absorption at $1600\text{--}1500\text{cm}^{-1}$ which is associated with ($\text{C}=\text{N}=\text{O}$) nitro amine and nitroso compounds ($\text{N}=\text{N}=\text{O}$). Also, present is the spectral absorption at $860\text{--}680\text{cm}^{-1}$, which is associated with aromatic CH stretching.

The absorption spectra generally show that DEMS and ATSP inhibitor molecules contain S, O and N constituents in their functional groups: ($\text{O}-\text{H}$, $\text{N}-\text{H}$, $\text{C}=\text{O}$, $\text{C}=\text{S}$, $\text{C}-\text{H}$ and $\text{N}=\text{O}$) and are likely sites for coordination with metal surfaces.

Gravimetric Method: Corrosion rate of mild steel as a function of exposure time: Values of weight loss of mild steel (expressed in grams) obtained after 3 hours immersion in 1.0M HCl after the introduction of the inhibitors, DEMS and ATSP were evaluated as expressed in equation-5.

$$\Delta W = W_1 - W_2 \quad (5)$$

Where: ΔW is the weight loss difference in grams, W_1 and W_2 are the measured weights of the coupons before and after the introduction of inhibitors respectively. Plots of weight loss versus immersion time at varying concentrations of the Schiff bases (inhibitors) were made and displayed in Figures-3 and 4.

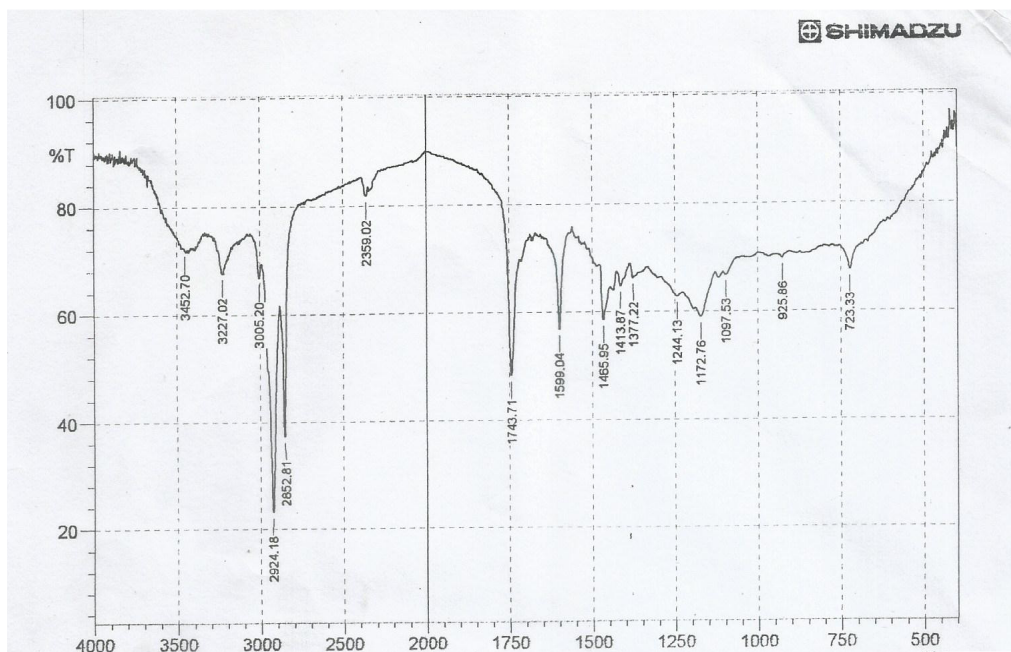


Figure-1: The FTIR spectrum of the synthesized Schiff base (DEMS).

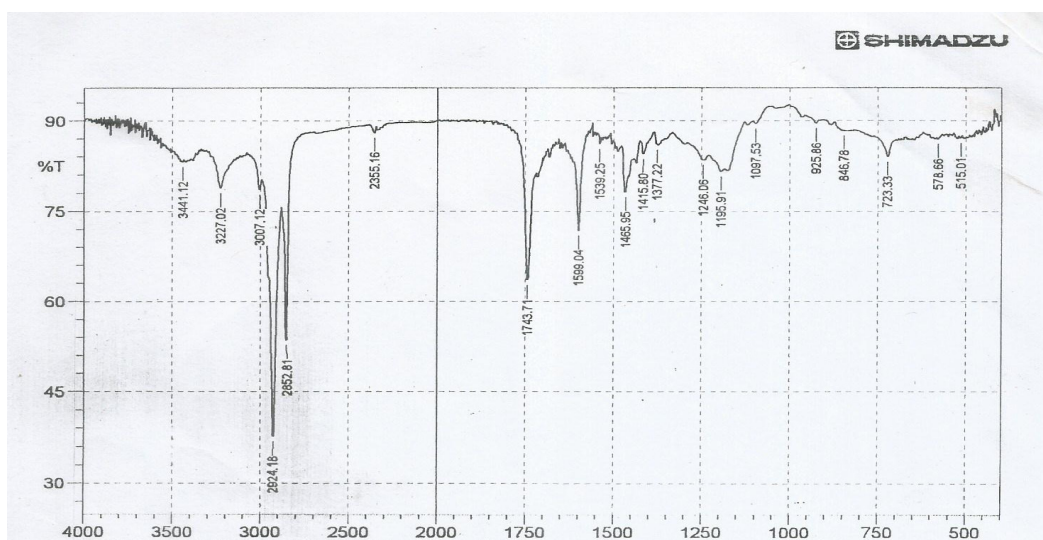


Figure-2: The FTIR spectrum of the synthesized Schiff base (ATSP).

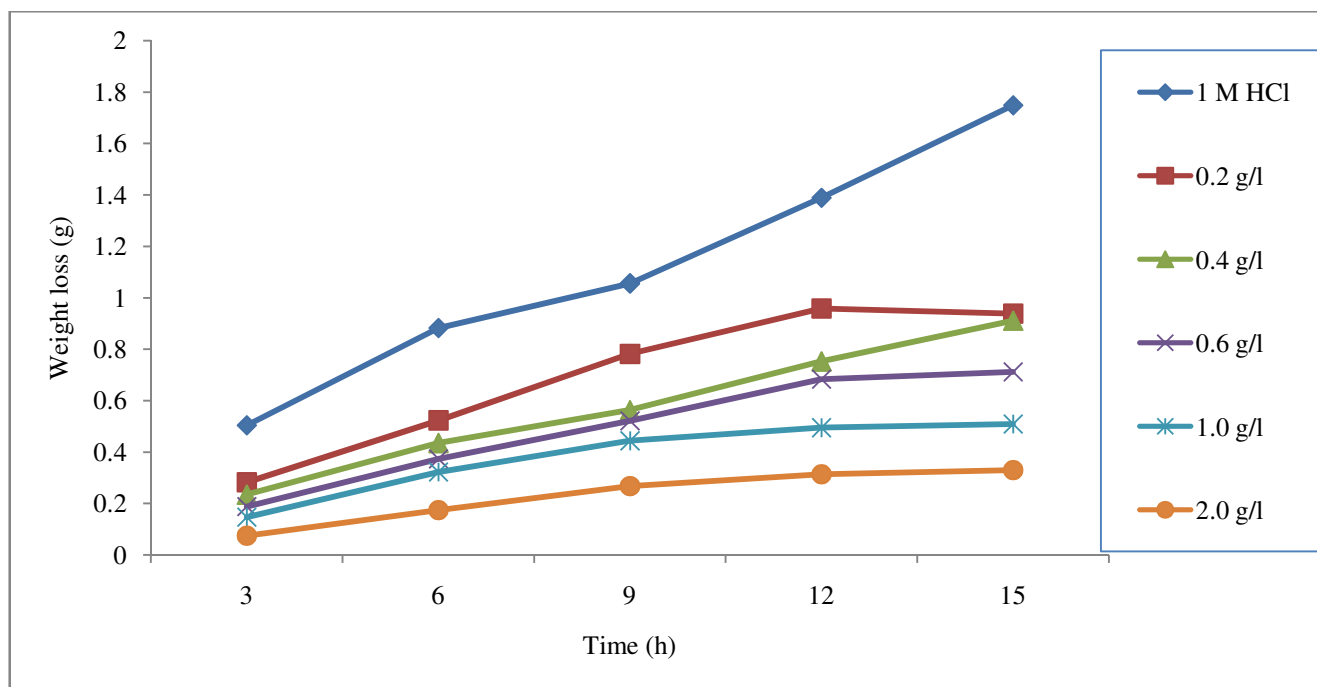


Figure-3: Weight loss (g) vs immersion time (h) in the blank and in varying concentrations of DEMS at 303 K.

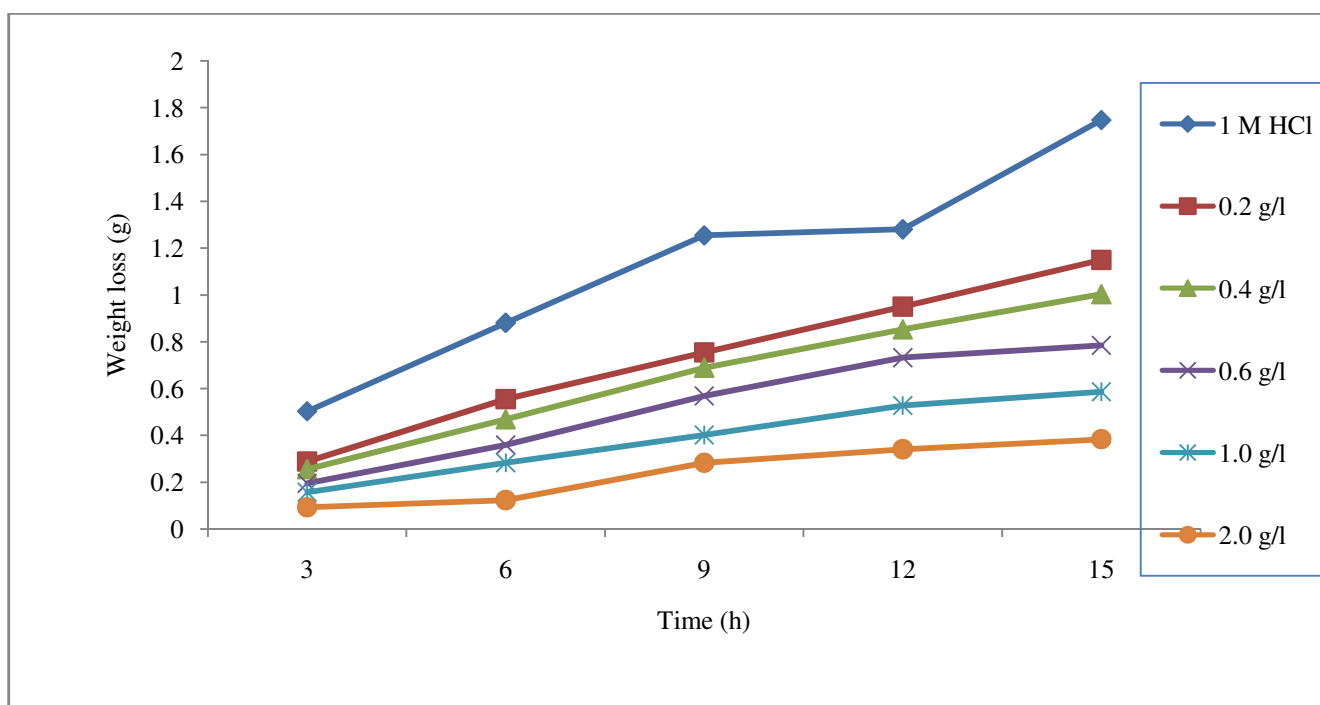


Figure-4: Weight loss (g) vs immersion time (h) in the blank and in varying concentrations of ATSP at 303 K.

These figures revealed that corrosion rate in the acid medium increases with a corresponding increase in immersion time from 3h-15h. The Schiff base inhibited mild steel exhibited decline in weight loss with a rise in concentration of the Schiff bases.

Corrosion rate and percentage inhibition as a function of inhibitor concentration: Even with varying concentrations of

the inhibitors, DEMS and ATSP in the acidic solution, slight weight losses were still observed on the mild steel.

Tables-1 and 2 display the corrosion rate (CR), surface coverage (θ) and percentage inhibition (I%) of the inhibitors at the expiration of 15h exposure time and at temperature ranges 303-343K.

Table-1: Corrosion rate (CR), surface coverage (θ) and percentage inhibition (I%) of the mild steel in 1.0M HCl in varying concentrations of DEMS at 303-343K.

303 K					313 K				
Inhibitor conc (g l ⁻¹)	Weight loss	(CR)	θ	I %	Inhibitor conc (g l ⁻¹)	Weight loss	(CR)	θ	I %
Blank	1.7476	0.0129	-	-	Blank	2.4321	0.018	-	-
0.2	0.9437	0.007	0.4600	46.00	0.2	1.4743	0.0109	0.3933	39.33
0.4	0.9108	0.0067	0.4788	47.88	0.4	1.318	0.0098	0.4576	45.76
0.6	0.7117	0.0053	0.5928	59.28	0.6	1.0894	0.0081	0.5517	55.17
1.0	0.5087	0.0038	0.7089	70.89	1.0	0.8113	0.006	0.6661	66.61
2.0	0.3296	0.0024	0.8114	81.14	2.0	0.5259	0.0039	0.7836	78.36
323 K					333 K				
Inhibitor conc (g l ⁻¹)	Weight loss	(CR)	θ	I %	Inhibitor conc (g l ⁻¹)	Weight loss	(CR)	θ	I %
Blank	5.6963	0.0422	-	-	Blank	5.9966	0.0444	-	-
0.2	3.8564	0.0286	0.32 1	32.31	0.2	4.4504	0.033	0.2575	25.75
0.4	3.4513	0.0256	0.3942	39.42	0.4	3.9973	0.0296	0.3331	33.31
0.6	2.7849	0.0206	0.5112	51.12	0.6	3.4849	0.0258	0.4186	41.86
1.0	2.1053	0.0156	0.6305	63.05	1.0	2.4532	0.0182	0.5907	59.07
2.0	1.5682	0.0116	0.7247	72.47	2.0	1.6806	0.0124	0.7196	71.96
343 K									
Inhibitor conc (g l ⁻¹)	Weight loss	(CR)	θ	I %					
Blank	6.001	0.0445	-	-					
0.2	4.9789	0.0369	0.1712	17.12					
0.4	3.9432	0.0292	0.3436	34.36					
0.6	3.6123	0.0268	0.3987	39.87					
1.0	3.0984	0.023	0.4842	48.42					
2.0	1.9682	0.0146	0.6724	67.24					

Table-2: Corrosion rate (CR), surface coverage (θ) and percentage inhibition (%) of the mild steel in 1.0M HCl in different concentrations of the inhibitor (ATSP) at 303-343K.

303K					313K			
Conc. g l ⁻¹	Weight loss	CR	θ	I%	Weight loss	CR	θ	I%
Blank	1.7476	0.0129			2.4321	0.018	-	-
0.2	1.1495	0.0085	0.3422	34.22	1.6482	0.0122	0.3223	32.23
0.4	0.9701	0.0072	0.4449	44.49	1.4279	0.0106	0.4129	41.29
0.6	0.7849	0.0058	0.5509	55.09	1.1708	0.0087	0.5186	51.86
1.0	0.5866	0.0043	0.6643	66.43	0.9052	0.0067	0.6278	62.78
2.0	0.3983	0.003	0.7721	77.21	0.6581	0.0049	0.7294	72.94
323K					333K			
Conc. g l ⁻¹	Weight loss	CR	θ	I%	Weight loss	CR	θ	I%
Blank	5.6963	0.0422	-	-	5.9966	0.044419	-	-
0.2	3.9381	0.0292	0.3087	30.87	4.5339	0.033584	0.2436	24.359
0.4	3.4519	0.0256	0.3941	39.41	3.9104	0.028966	0.3476	34.761
0.6	2.8376	0.021	0.5019	50.19	3.6355	0.02693	0.3935	39.348
1.0	2.2594	0.0167	0.6034	60.34	2.5409	0.018821	0.5761	57.609
2.0	1.7342	0.0128	0.6956	69.56	1.8762	0.013898	0.687	68.699
343 K								
Conc. g l ⁻¹	Weight loss		CR		θ		I%	
Blank	6.001		0.0445		-		-	
0.2	5.0011		0.037		0.1675		16.75	
0.4	4.4231		0.0328		0.2637		26.37	
0.6	3.8743		0.0287		0.3551		35.51	
1.0	3.4101		0.0253		0.4324		43.24	
2.0	2.1935		0.0162		0.6349		63.49	

Results showed a decline in weight loss and a corresponding increase in inhibitory performance (% E) as concentrations of the inhibitors (DEMS and ATSP) gradually build up. The obtained results suggest that the employed inhibitors suppressed the corrosion rate and a similar interpretation had been supported by the work of Eddy¹¹. This observation may be

explained to have resulted from the creation of a strong barrier between the metal surface under study and the HCl aqueous solution as the inhibitor molecules gradually adsorbed onto the metal surfaces leading to a retardation in the metal deterioration¹².

Temperature influence on rate of corrosion and percentage Inhibition: The influence of temperature on the extent of inhibition of mild steel corrosion by DEMS and ATSP was estimated from the measured values of the weight loss at the selected study temperature ranges of 303K to 343K and at varying concentrations of the inhibitors as shown in Table 1 and Table-2. The tables show that for both inhibitors, CR increased with a rise in temperature from 303K to 343K and this may have resulted from the increase in solubility of the protective covering on the surfaces of the mild steel with a rise in temperature and a similar interpretation had been given¹³. Corrosion rates as the inhibitors, DEMS and ATSP were added were much lower than the values evaluated without the inhibitors for each temperature studied. Also, The calculated values of the percentage inhibition (I %) as shown in Tables-1 and 2 revealed that their inhibition performances increased steeply as concentrations of the inhibitors increased.

Activation Energy (E_a) for the Corrosion Process: The activation energy for the inhibition process was evaluated using the Arrhenius equation. The equation explained that the rate of corrosion of metals varies exponentially with the reciprocal of temperature and is expressed in Equation-6.

$$\log CR = \log A - \frac{E_a}{2.303RT} \quad (6)$$

E_a is the activation energy, R is the universal gas constant, T is the absolute temperature in Kelvin and A is the Arrhenius pre-exponential factor. From Equation-6, plots of $\log (CR)$ vs $1/T$ yielded straight lines for the corrosion control using both inhibitors as shown in Figures-5 and 6. The activation energy is evaluated from the slope of the linear plots and displayed in Tables-3 and 4.

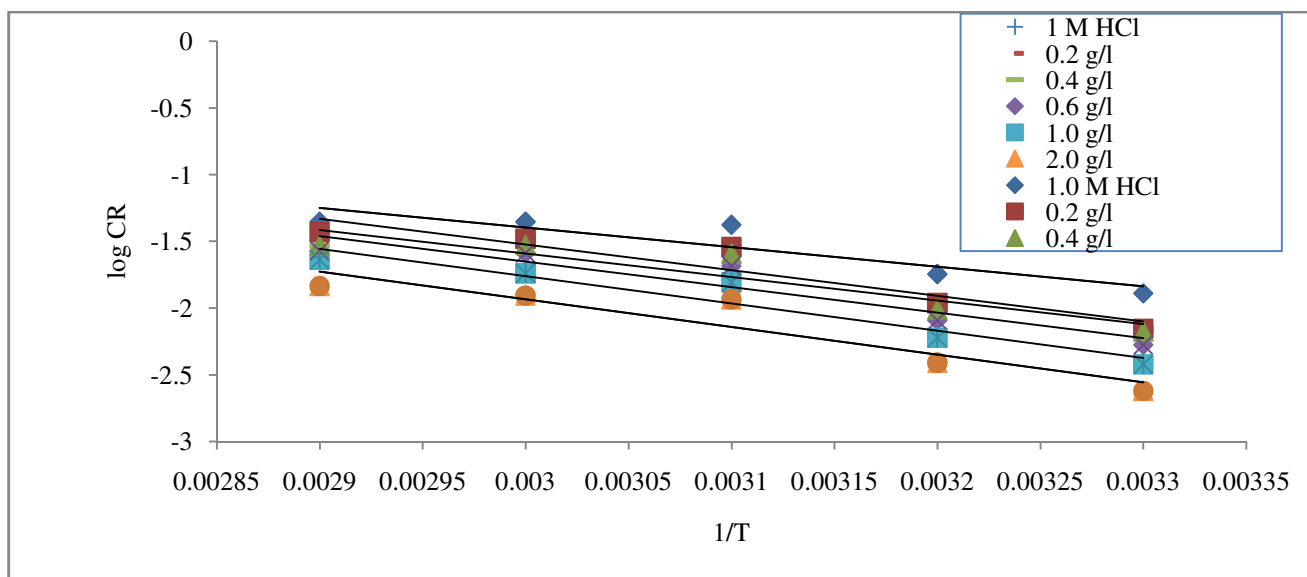


Figure-5: Variation of log CR with $1/T$ for the inhibition process using varying concentrations of DEMS.

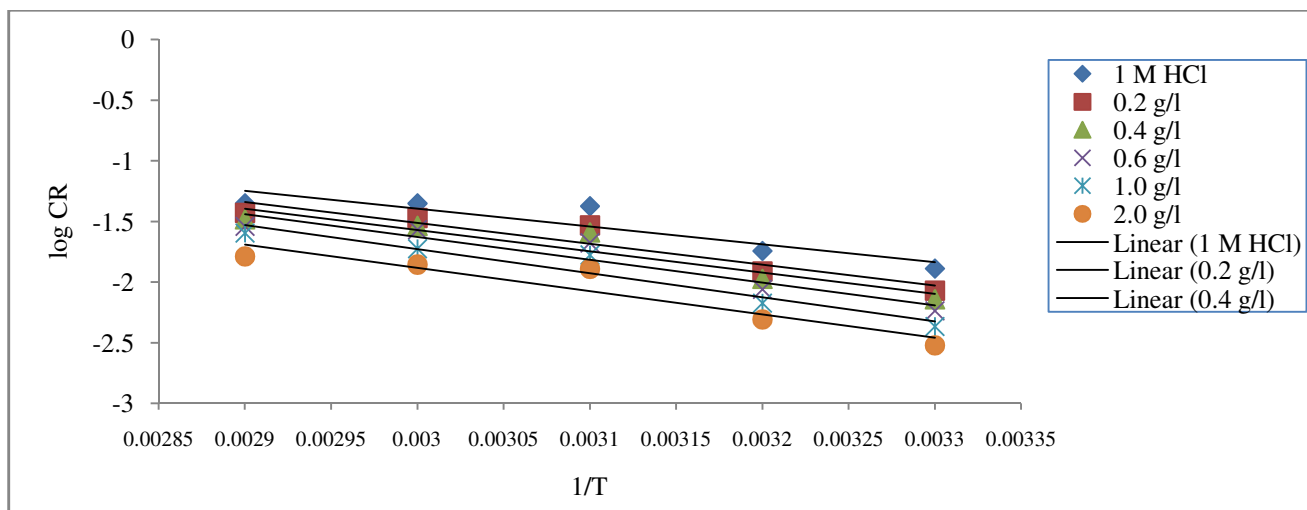


Figure-6: Variation of log CR with $1/T$ for the inhibition process using varying concentrations of ATSP.

The results show in Table-3 and 4 that the E_a values calculated when the inhibitors were applied were greater than those of the uninhibited system. Also, values of E_a for the inhibited solution increased with rise in concentration of the inhibitors and these accounted for the increased inhibition performance as concentration gradually build up. The deterioration of the mild steel in the presence of the inhibitors, DEMS and ATSP were slow due to the high activation energy values calculated and that lead to low corrosion rate.

This observation could be interpreted to result from the formation of protective covering on the mild steel surface as concentrations of the inhibitors increased. The increase in values of activation energy observed as temperature increased

show that the percentage inhibition decreases with temperature and a similar observation had been reported¹⁴.

Activation parameters for the corrosion process: The transition state equation was employed to evaluate the enthalpy of adsorption (ΔH_{ads}) and entropy of adsorption (ΔS_{ads}) and values obtained from these could be used to estimate the free Energy of adsorption (ΔG_{ads}) at a given temperature. The transition-state equation relates the activation parameters viz; ΔH_{ads} and ΔS_{ads} to corrosion rate of the metal coupons¹⁵⁻¹⁷. Linear plots of $\log CR/T$ against reciprocal of the temperature were obtained and displayed in Figures-7 and 8, and from the slope and intercept of such plots, values of ΔH_{ads} and ΔS_{ads} were obtained and presented in Tables-5 and 6.

Table-3: Activation energy, (E_a) values for the inhibition process using DEMS.

Conc. of inhibitor (g/l)	$E_{a303\text{ K}}$ (kJ mol ⁻¹)	$E_{a313\text{ K}}$ (kJ mol ⁻¹)	$E_{a323\text{ K}}$ (kJ mol ⁻¹)	$E_{a333\text{ K}}$ (kJ mol ⁻¹)	$E_{a343\text{ K}}$ (kJ mol ⁻¹)
1M HCl	3697.34	3819.37	3941.39	4063.42	4185.44
0.2g/l	4849.1	5009.13	5169.17	5329.2	5489.24
0.4g/l	4430.42	4576.63	4722.85	4869.07	5015.29
0.6g/l	4813.83	4972.7	5131.57	5290.45	5449.32
1.0g/l	5153.66	5323.75	5493.84	5663.92	5834.01
2.0g/l	5216.14	5388.29	5560.43	5732.58	5904.73

Table-4: Activation energy, (E_a) values for the inhibition process using ATSP.

Conc. of inhibitor (g/l)	$E_{a303\text{ K}}$ (kJ mol ⁻¹)	$E_{a313\text{ K}}$ (kJ mol ⁻¹)	$E_{a323\text{ K}}$ (kJ mol ⁻¹)	$E_{a333\text{ K}}$ (kJ mol ⁻¹)	$E_{a343\text{ K}}$ (kJ mol ⁻¹)
1M HCl	3697.6	3819.63	3941.66	4063.7	4185.73
0.2g/l	4326.12	4468.9	4611.68	4754.45	4897.23
0.4g/l	4417.82	4563.62	4709.42	4855.23	5001.03
0.6g/l	4734.98	4891.25	5047.52	5203.79	5360.06
1.0g/l	5007.8	5173.08	5338.35	5503.62	5668.9
2.0g/l	4830.45	4989.88	5149.3	5308.72	5468.14

Table-5: Thermodynamic variables for the mild steel inhibition process using DEMS.

Inhibitor conc. (g/l)	ΔH_{ads} (kJ/mol)	ΔS_{ads} (J/mol/K)	ΔG_{ads} (kJ/mol)
1M HCl (blank)	30.79	-98.95	-
0.2 g l ⁻¹	39.54	-75.11	-13.77
0.4g l ⁻¹	36.36	-85.99	-12.21
0.6 g l ⁻¹	39.27	-78.39	-12.35
1.0 g l ⁻¹	41.86	-72.73	-12.36
2. 0g l ⁻¹	42.33	-74.62	-12.05

Table-6: Thermodynamic variables for the mild steel inhibition process using ATSP.

Inhibitor conc. (g/l)	ΔH_{ads} (kJ/mol)	ΔS_{ads} (J/mol/K)	ΔG_{ads} (kJ/mol)
1M HCl (blank)	30.79	-98.94	-
0.2 g l ⁻¹	35.57	-86.85	-12.53
0.4g l ⁻¹	36.26	-85.87	-11.87
0.6 g l ⁻¹	38.66	-79.76	-11.92
1.0 g l ⁻¹	40.75	-75.45	-11.84
2. 0g l ⁻¹	39.40	-82.43	-11.45

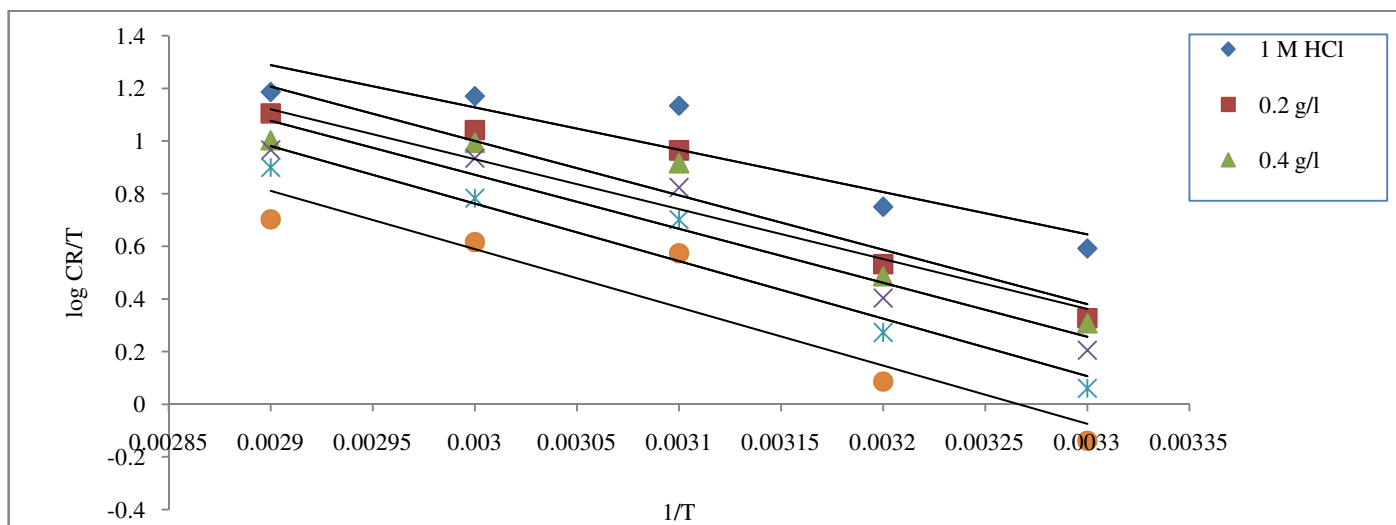


Figure-7: Variation of log CR/T vs 1/T for the mild steel corrosion inhibition in 1.0M HCl containing various concentrations of DEMS.

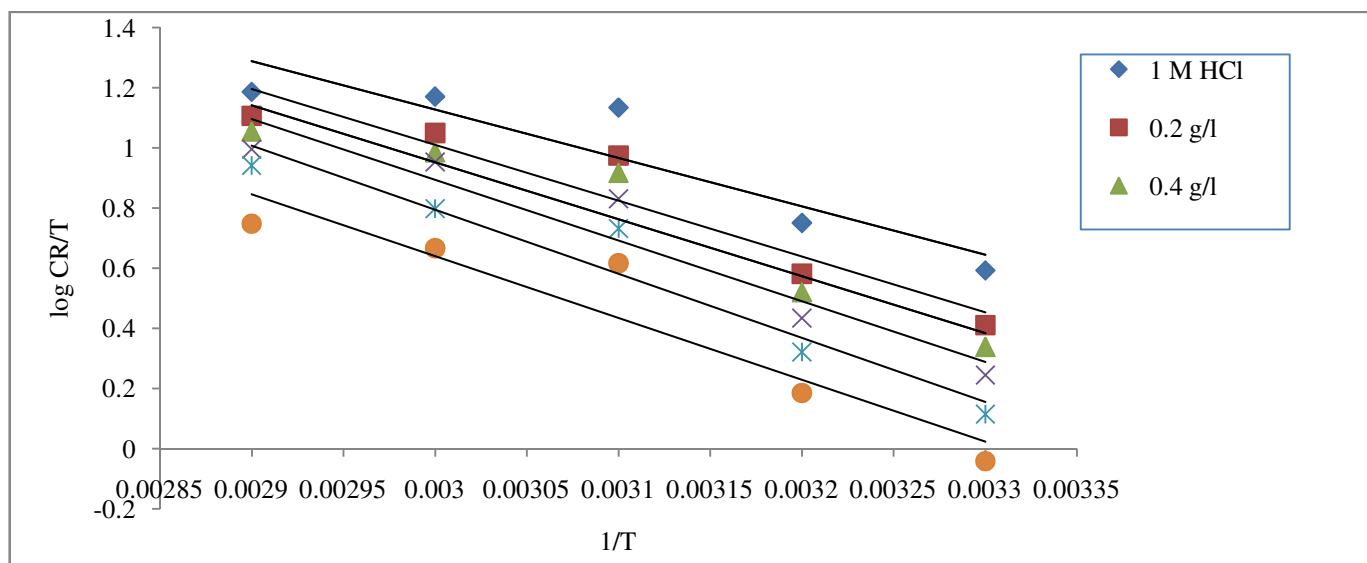


Figure-8: Variation of log (CR/T) vs 1/T for the mild steel corrosion inhibition in 1.0 M HCl containing various concentrations of ATSP.

The positive values of ΔH_{ads} denote the endothermic nature of the corrosion inhibition process. The negative values of ΔS_{ads} as shown in Tables-5 and 6 indicate decreasing freedom (or disorderliness) at the mild steel-inhibitor interface as concentrations of DEMS and ATSP increased. The Gibbs free energy of adsorption (ΔG_{ads}) was calculated using the relation shown in equation-7.

$$\Delta G_{\text{ads}} = -RT \ln (55.5K_{\text{ads}}) \quad (7)$$

The negative values of ΔG_{ads} as shown in Tables-5 and 6 give an indication of strong bonding between the inhibitor molecules and the corroding specimen and a similar observation had been reported¹⁸. The calculated values of ΔG_{ads} , which were less than -20 kJ mol^{-1} , further indicate that the mode of bonding of the inhibitors (DEMS and ATSP) followed physisorption.

Adsorption Isotherms: Equilibrium adsorption Isotherms are vital for estimating the likely mechanism of electrochemical reactions such as corrosion¹⁹. They aid in explanation of the nature of attraction between the corroding metal specimen and an inhibitor during corrosion control.

Two adsorption isotherms namely: Temkin and Langmuir were employed in the present study.

Temkin Adsorption Isotherm: Temkin adsorption isotherm is quite applicable to systems where there are strong chemical interactions between the inhibiting species and the corroding metal. Plot of θ versus $\log C$ yielded straight lines in the present study as shown in Figures-9 and 10.

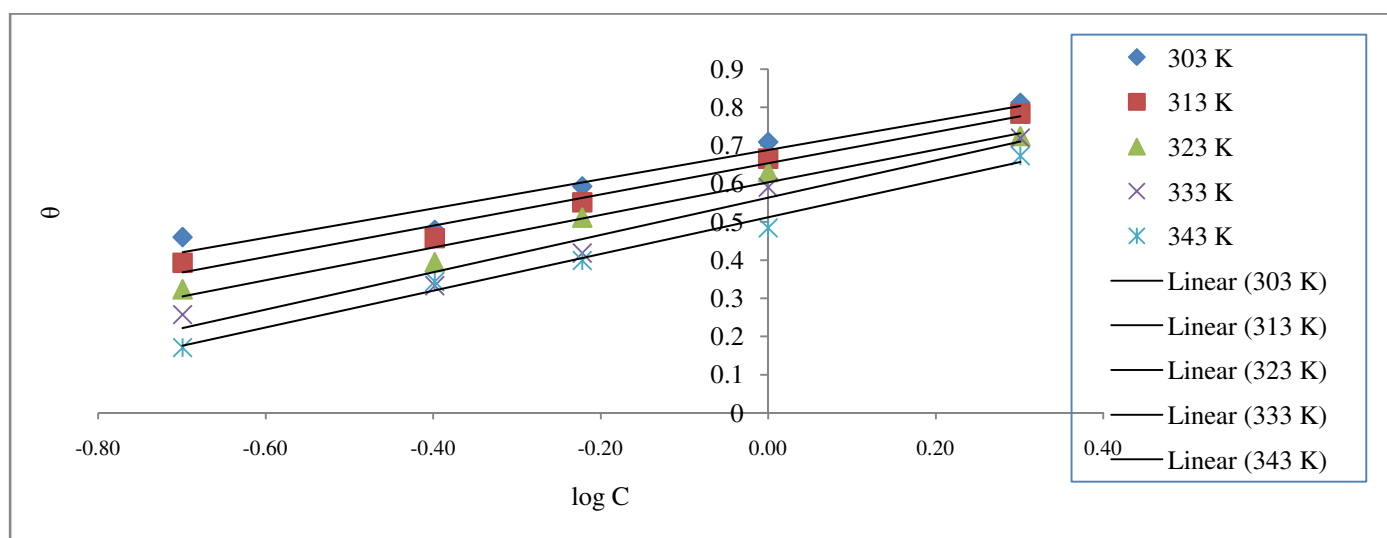


Figure-9: Plots of θ vs $\log C$ according to Temkin for the inhibitory action of DEMS on the mild steel specimen at various temperatures.

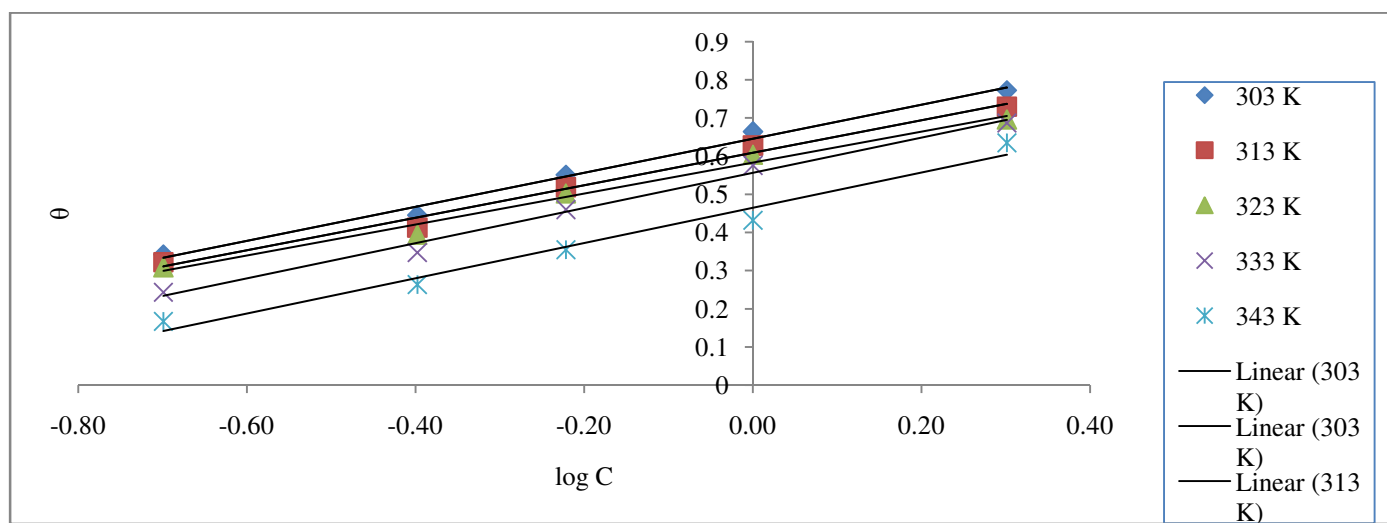


Figure-10: Plots of θ vs $\log C$ according to Temkin for the inhibitory action of ATSP on the mild steel specimen at various temperatures.

The Langmuir: For an experimental corrosion inhibition data to fit into Langmuir isotherm, a plot of $\log C/\theta$ versus $\log C$ must be linear. Figures-11 and 12 depict Langmuir isotherm plots for the adsorption of DEMS and ATSP on the mild steel surface. The linear plots of $\log (C/\theta)$ versus $\log C$ obtained for both inhibitors (DEMS and ATSP) in the current study were indicators of good fit of the corrosion data into the isotherm.

Potentiodynamic Polarisation measurement: The Tafel polarisation curves display clearly the cathodic and anodic polarization regions of the electrochemical assembly. The shapes of the Tafel plots were unchanged as the inhibitors were applied in the same way as their absence except that the plots bent towards lower current density with the rise in concentration

of the inhibitors. This shows that the Schiff bases, DEMS and ATSP retarded the corrosion process as their concentrations increased, and yet maintained the mechanism of the corrosion process in the acidic medium. Figures-13 and 14 show the Tafel curves at varying concentrations of the inhibitors, DEMS and ATSP. The Figures-13 and 14 show that the inhibitor molecules influenced reactions at the cathodic and anodic ends as observed from the slight changes in the E_{corr} values obtained from the plots. Table-7 shows values of the electrochemical parameters estimated from extrapolated Tafel lines of Figures-12 and 13. These electrochemical parameters include: anodic and cathodic Tafel slopes (b_a and b_c), corrosion current density (I_{corr}) and the corrosion potential (E_{corr}).

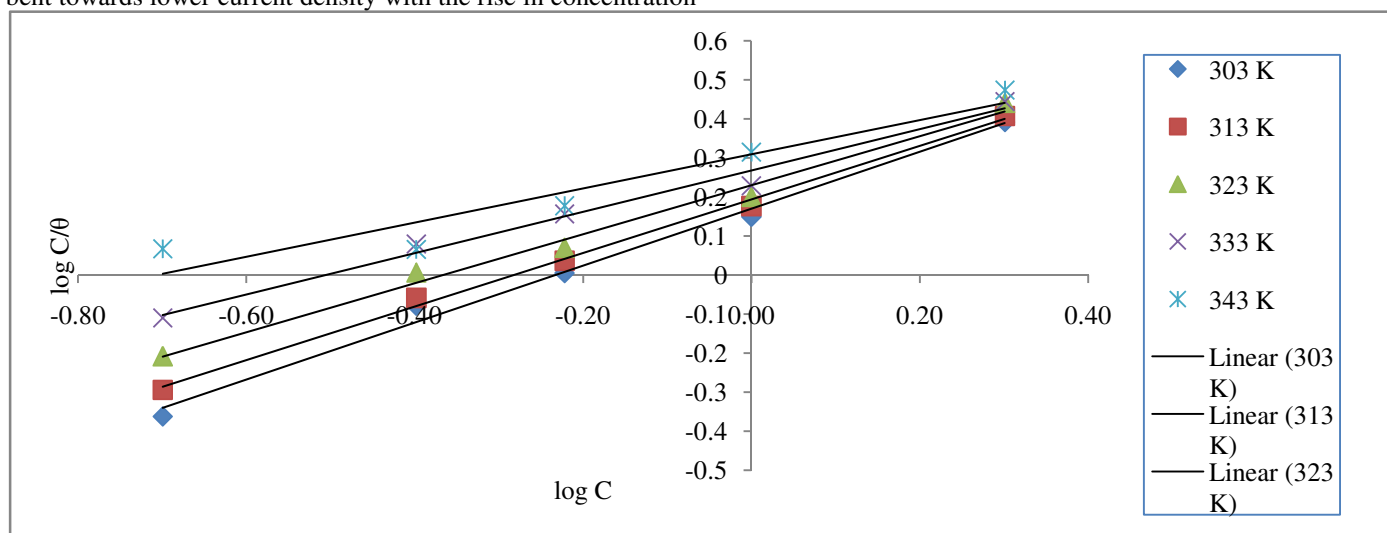


Figure-11: Plots of $\log C/\theta$ vs $\log C$ according to Langmuir for the inhibitory action of DEMS on the mild steel coupons at various temperatures.

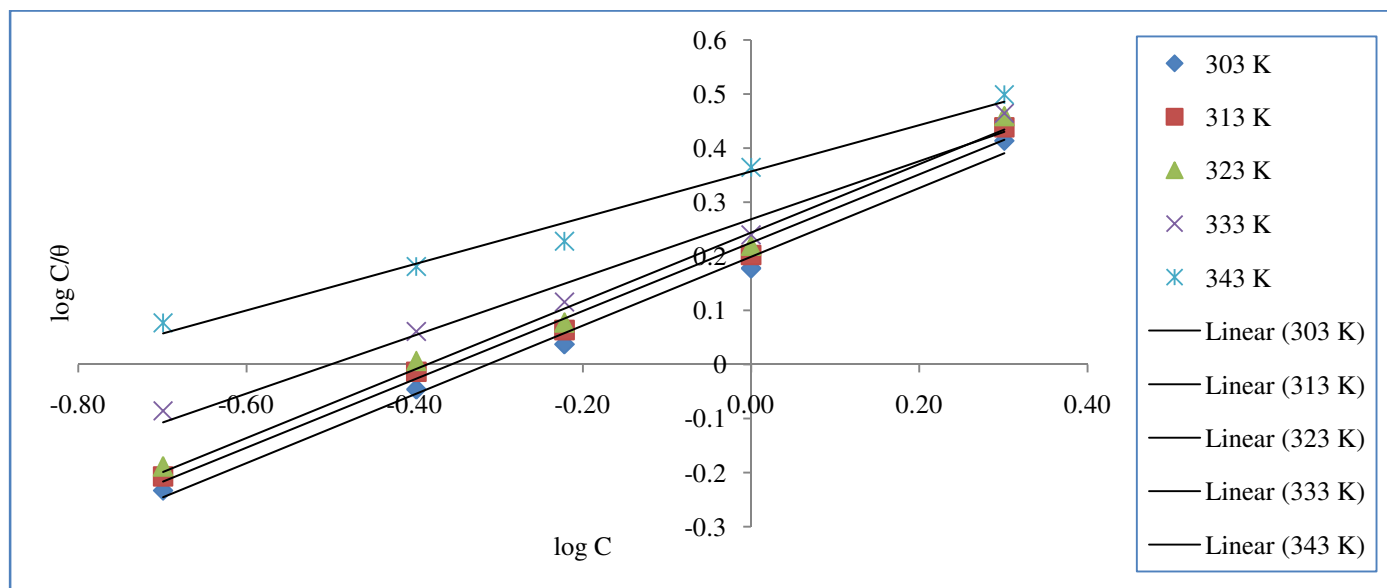


Figure-12: Plots of $\log C/\theta$ vs $\log C$ according to Langmuir for the inhibitory action of ATSP on the mild steel coupons at various temperatures.

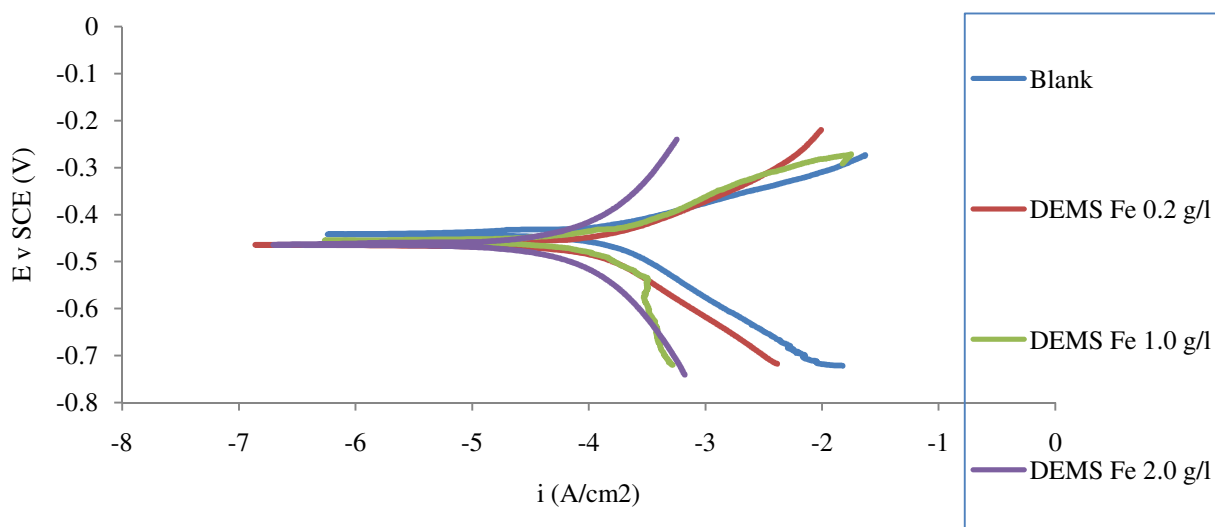


Figure-13: Tafel polarization plots for mild steel corrosion inhibition in 1M HCl in varying concentrations of DEMS at 303K.

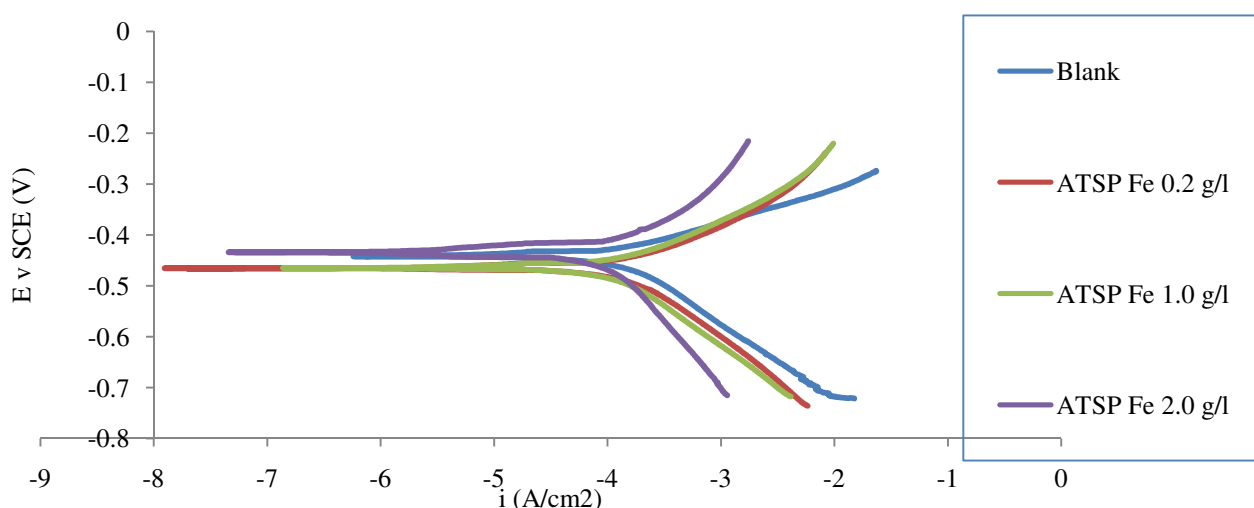


Figure-14: Tafel polarization plots for mild steel corrosion inhibition in 1M HCl in varying concentrations of ATSP at 303K.

Table-7: Electrochemical kinetic values obtained from potentiodynamic polarisation plots at different concentrations of DEMS and ATSP.

Inhibitors	Conc. g/l	E_{corr} (mV/SCE)	I_{corr} (μAcm^{-2})	b_c (mVdec ⁻¹)	b_a (mVdec ⁻¹)	I %
DEMS	0.00	-442	570	331	615	-
	0.2	-465	319	398	628	44.03
	1.0	-455	186	318	641	67.37
	2.0	-465	76	365	670	86.60
ATSP	0.2	-466	375	343	646	34.03
	1.0	-465	202	321	630	64.56
	2.0	-443	158	335	643	72.28

It could be observed from Table-7, that there was a fall in I_{corr} value as concentrations of DEM and ATSP increased and this led to a corresponding rise in percentage inhibition (I%). The observed fall in I_{corr} value shows that the inhibitors suppressed corrosion reactions at the cathodic and anodic regions through their adsorption onto the cathodic and anodic sites. The deviations in E_{corr} from Table-7 were less than $\pm 85\text{mV/SCE}$ when compared to E_{corr} of the blank and based on this; the inhibitors could be regarded as mixed type. From values obtained in Table-7, the inhibitor DEMS is observed to inhibit more than the inhibitor, ATSP.

Conclusion

The study of the inhibition potentials of two Schiff bases synthesized from carboxylic acids (Linoleic and Benheric acids) :2[(2-diethylamino) ethylmethyl amino]-4-methyl-5-3(3-methyl sulfanyl propyl amino) methylidene cyclohexdien-1-one (DEMS) and 1- (azepan-1-yl)-2-[4-(2-tert-butyl sulfanylethyl piperazin] ethanone (ATSP) shows that the Schiff bases are effective inhibitors against mild steel corrosion in 1.0 M HCl. The FT-IR spectra showed that the studied Schiff bases contained N, O and S atoms in addition to their π – electrons and these may be responsible for their high inhibition performance. The gravimetric technique shows that inhibition efficiencies increased with a rise in concentrations of DEMS and ATSP but decreased with a fall in temperature of the system and this signifies that physisorption may likely be the predominant mode of the adsorption process. The Langmuir isotherm was found to give the best interpretation to the experimental corrosion inhibition data with R^2 values of 0.99. Thermodynamically, the calculated negative entropy values (ΔS_{ads}) for the inhibition process depict decreasing degree of disorderliness as the concentration of the inhibitors increased. Also, the negative low values of free energy of adsorption (ΔG_{ads} values less than 20kJ mol^{-1}) indicate that the mode of bonding of the two Schiff base inhibitors followed physisorption. The nature of the Tafel polarization curves shows that the inhibitors are of mixed type, affecting reaction at both anodic and cathodic sites.

References

1. Liu P., Fang X., Tang Y., Sun C. and Yao C. (2001). Electrochemical and quantum chemical studies of 5-substituted tetrazoles as corrosion inhibitor for copper aerated 0.5 M H_2SO_4 solution. *Materials Science and Application*, 2, 1268-1278.
2. Achary G., Sachin H.P., Naik Y.A. and Venkatesha T.V. (2008). The corrosion inhibition of mild steel by 3-formyl-8- hydroxyquinoline in hydrochloric acid medium. *Material Chemistry and Physics*, 107, 44-50.
3. Quraishi M.A., Ahamad I., Singh A.K., Shukla S.K., Lai B and Singh V. (2008). N- (Piperidinomethyl)-3-Ecpyridylidene amino, a new and effective acid corrosion inhibitor for mild Steel. *Material Chemistry and Physics*, 112, 1035-1039.
4. Umoren S.A., Obot I.B. and Ebenso E.E. (2008). Corrosion Inhibition of aluminium using exudates gum from *Pachylobus edulis* in the presence of halide ions in HCl. *Electron, Journal of Chemistry*, 5(2), 355-364.
5. Eddy N.O. (2011). Experimental and theoretical studies of some amino acids and their potential activity as inhibitors for the corrosion of mild steel. Part 2. *Journal for Advance Research*, 2, 35-47.
6. Ita B.I. (2004). A study of corrosion inhibition of mild steel in 0.1 M hydrochloric acid by O-vanillin and O-vanillin hydrazone. *Bulletin of Electrochistry*, 20(8), 363-370.
7. Hosseini S.M.A., Eftekhar S and Amiri M. (2007). Polarisation behavior of stainless steel type 302 in HCl solution of benzotriazole. *Asian Journal of Chemistry*, 19(4), 2574-2580.
8. Eddy N.O. and Odoemelam S.A. (2008). Inhibition of the corrosion of mild steel in acid medium by penicillin V. Potassium. *Advances in Natural and Applied Sciences*, 2(3), 225-232.
9. Toliwal S.D., Kalpesh J. and Pavagadhi T. (2010). Inhibition of corrosion of mild steel in HCl solution by Schiff base derived from non-traditional oils. *Journals of Applied Chemical Research*, 12, 24-36.
10. Yassen A.A., Najim A. and AL-Masoudi A. (2003). A new class of dihaloquinolones bearing Naldehydoglycosyl hydrides, mercaptol, 1,2,4- triazole, oxadiazoline and a-amino ester precursor: synthesis and anti-microbial activity. *Journal of Brazil Chemical Society*, 14, 790-796.
11. Eddy N.O. (2011). Experimental and theoretical studies of some amino acids and their potential activity as inhibitors for the corrosion of mild steel, Part 2. *Journal for Advance Research*, 2, 35-47.
12. Ezeoke A.U., Adeyemi O.G., Akerele O.A and Obi-Egbedi N.O. (2012). Computational and experimental studies of 4-amino antipyrine as corrosion inhibitor for mild steel in sulphuric acid solution. *International Journal of Electrochemical Sciences*, 7, 534-553.
13. Okafor P.C., Ebenso E.E. and Ekpe U. (2004). Inhibition of the acid corrosion of aluminium by some derivatives of thiosemicarbazone. *Bulletin of Chemical Society of Ethiopia*, 18(2), 181-192.
14. Stern I. and Martinez S. (2005). An inhibitory of lo-carbon steel by mimosa tannin in sulphuric acid solution. *Journal of Electrochemical*, 31, 973-978.
15. Asshassi-Sorkhabi H., Shabani B. and Seifzadeh D. (2005). Corrosion Inhibition of mild steel by some Schiff base compounds in HCl. *Applied Surface Science*, 239, 154-164.

16. Yurt A., Balaban A., Kandemer S.U., Bereket G. and Erk B. (2004). Investigation of some Schiff bases as HCl corrosion inhibitors for carbon steel. *Material Chemistry and Physics*, 85, 420-426.
17. Yurt A., Bekeret G., Rivrak A., Balaban A and Erk B. (2005). Effect of Schiff bases containing pyridyl group as corrosion inhibitors for low carbon steel and in 0.1M HCl. *Journal of Applied Electrochem.*, 35, 1025-1032.
18. Upadhyay R.K. and Mathur S.P. (2007). Effect of Schiff bases as corrosion inhibitors of mild steel in sulphuric acid. *E-Journal of Chemistry*, 4(3), 408-414.
19. Emergul K.C., Kurtaran R. and Atakol O. (2003). An Investigation of Chloride-Substituted Schiff bases as corrosion inhibitors for mild steel. *Journal of Corrosion Science*, 45, 2803-2817.